Reemergence of Anthropogenic Carbon Into the Ocean's Mixed Layer Strongly Amplifies Transient Climate Sensitivity

Keith B. Rodgers, S. Schlunegger, Richard D. Slater, Masao Ishii, T. L. Frölicher, Katsuya Toyama, Yves Plancherel, Olivier Aumont, A. J. Fassbender

Geophysical Research Letters

RESEARCH LETTER
10.1029/2020GL089275

Key Points:
- Marine chemistry-climate feedbacks plan an important role in determining climate sensitivity
- The rate of reemergence of anthropogenic carbon plays an important role in determining climate sensitivity
- The sensitivity identified here to perturbations to the buffering capacity of CO_2 in seawater is larger than that emphasized in IPCC AR5

Correspondence to:
K. B. Rodgers,
krodgers@pusan.ac.kr

Citation:
Rodgers, K. B., Schlunegger, S., Slater, R. D., Ishii, M., Frölicher, T. L., Toyama, K., et al. (2020). Reemergence of anthropogenic carbon into the ocean's mixed layer strongly amplifies transient climate sensitivity. *Geophysical Research Letters*, *47*, e2020GL089275. https://doi.org/10.1029/2020GL089275

Received 25 JUN 2020
Accepted 26 AUG 2020
Accepted article online 2 SEP 2020

Reemergence of Anthropogenic Carbon Into the Ocean's Mixed Layer Strongly Amplifies Transient Climate Sensitivity

K. B. Rodgers[1,2], S. Schlunegger[3], R. D. Slater[3], M. Ishii[4], T. L. Frölicher[5,6], K. Toyama[4], Y. Plancherel[7], O. Aumont[8], and A. J. Fassbender[9]

[1]Center for Climate Physics, Institute for Basic Science, Busan, South Korea, [2]Pusan National University, Busan, South Korea, [3]Program in Atmospheric and Oceanic Sciences, Princeton University, Princeton, NJ, USA, [4]Climate and Geochemistry Research Department, Meteorological Research Institute, Japan Meteorological Agency, Tsukuba, Japan, [5]Climate and Environmental Physics, Physics Institute, University of Bern, Bern, Switzerland, [6]Oeschger Centre for Climate Change Research, University of Bern, Bern, Switzerland, [7]The Grantham Institute for Climate Change, Imperial College London, London, UK, [8]Sorbonne Universités, UPMC, Université Paris 06-CNRS-IRD-NHNH, LOCEAN/IPSL, Paris, France, [9]Monterey Bay Aquarium Research Institute, Moss Landing, CA, USA

Abstract A positive marine chemistry-climate feedback was originally proposed by Revelle and Suess (1957, https://doi.org/10.3402/tellusa.v9i1.9075), whereby the invasion flux of anthropogenic carbon into the ocean serves to inhibit future marine CO_2 uptake through reductions to the buffering capacity of surface seawater. Here we use an ocean circulation-carbon cycle model to identify an upper limit on the impact of reemergence of anthropogenic carbon into the ocean's mixed layer on the cumulative airborne fraction of CO_2 in the atmosphere. We find under an RCP8.5 emissions pathway (with steady circulation) that the cumulative airborne fraction of CO_2 has a sevenfold reduction by 2100 when the CO_2 buffering capacity of surface seawater is maintained at preindustrial levels. Our results indicate that the effect of reemergence of anthropogenic carbon into the mixed layer on the buffering capacity of CO_2 amplifies the transient climate sensitivity of the Earth system.

1. Introduction

A priority in climate research is to quantify and constrain the transient climate response to cumulative emissions (TCRE; e.g., Matthews et al., 2009). The TCRE is often used to calculate the suite of remaining carbon budgets that define the allowable future carbon dioxide gas (CO_2) or equivalent emissions which are consistent with meeting climate targets such as those of the Paris Agreement (Collins et al., 2013; Rogelj et al., 2019). Estimates of the TCRE are subject to large uncertainties, as there are large intermodel differences (Gillet et al., 2013; Williams et al., 2019). To date efforts that focus on physical feedbacks and carbon cycle feedbacks have often been considered separately (Forster et al., 2013; Friedlingstein et al., 2006; Goodwin et al., 2015). The study of Katavouta et al. (2018) has posited that as much as half of TCRE is due to marine CO_2 buffering changes under sustained emissions, implying that differences in the magnitude of surface CO_2 buffering capacity changes in models may also contribute to intermodel differences.

Is the invasion flux of anthropogenic carbon (C_{ant}) into the global ocean, in the absence of perturbations to the physical state of the ocean, sufficient to sustain significant carbon concentration-climate feedbacks? As a complement to the more extensive analyses that have previously been devoted to describing changes associated with processes that occur through physical state perturbations (Friedlingstein et al., 2003, 2006), our goal here is to evaluate the relative importance of chemical processes (Bolin & Eriksson, 1959; Revelle & Suess, 1957) that require only the invasion flux of CO_2 itself to modify the strength of the ocean carbon sink.

Here we revisit the hypothesis proposed by Toyama et al. (2017), namely, that large sustained reemergence of C_{ant} from the ocean interior into the ocean's mixed layer can have an important impact on C_{ant} uptake by the ocean, through changes in the CO_2 buffering capacity of ocean surface waters. Toyama et al. (2017) applied a forward ocean circulation/carbon cycle model (the ORCA2 configuration of NEMO-PISCES) with a simulation forced at the surface with climatological atmospheric forcing fields and confirmed that at the

time of the World Ocean Circulation Experiment observations, centered on 1995, the net globally integrated annual mean uptake of C_{ant} by gas exchange was 2.04 PgC/yr. However, they also showed that the net upward and downward fluxes of C_{ant} across the base of the ocean's mixed layer were larger, with a net C_{ant} subduction (downward) flux of 4.96 PgC/yr and a net obduction (upward) flux of 4.50 PgC/yr. As a residual of the air-sea fluxes and net downward fluxes, and accounting for a mixed layer accumulation rate of 0.18 PgC/yr, a net downward diffusive C_{ant} transfer out of the mixed layer in 1995 of 1.4 PgC/yr was identified. They also presented a scaling argument based on Lagrangian calculations emphasizing that the median global ocean interior transit time for obducting (upward relative to the mixed layer base) water parcels is 10 yr, with this being significantly shorter than the characteristic time scale $\tau = 45$ yr for exponential increases in atmospheric CO_2. Thus, reemergence of C_{ant} into the mixed layer could induce a transient decline in the CO_2 buffering capacity of surface waters, reducing the ocean's ability to absorb excess CO_2.

As a step toward an explicit quantification of the effect of reemergence of C_{ant} into the mixed layer from below on the uptake of C_{ant} from the atmosphere, we have designed an idealized suite of runs with a forced ocean circulation-carbon cycle (MOM5-BLING, Galbraith et al., 2011; Griffies, 2009). The idealized conceptual model we impose is through a preindustrial carbonate chemistry state for the surface ocean via data override for the calculation of CO_2 partial pressure (pCO_2) in the gas exchange routines for the surface ocean layer. The Revelle factor of surface waters is maintained at its preindustrial level in our sensitivity experiment with the forward model. More specifically, we consider the case where the anthropogenic transients in sea surface dissolved inorganic carbon (DIC) and total alkalinity (TA) are suppressed under a historical/RCP8.5 emissions pathway. We consider this to be a strong and idealized perturbation appropriate for testing the sensitivity of ocean uptake of C_{ant} for the case of an ocean without reemergence from the permanent pycnocline of C_{ant}. In other words, we assume that all obducting water masses are from interior reservoirs with no memory of the anthropogenic transient in atmospheric CO_2, and we simultaneously assume that all C_{ant} entering the mixed layer via gas exchange is instantaneously subducted.

2. Methods

2.1. Idealized Modeling Analyses of the Impact of Reemergence on Ocean CO_2 Uptake

We conduct three simulations here. First, a preindustrial control run is conducted with zero CO_2 emissions (PI). In addition, two simulations with historical/RCP8.5 CO_2 emissions pathways (van Vuuren et al., 2011) are performed with a forward ocean circulation-carbon cycle model imposing a fixed physical climate (with repeated seasonal variations). In this way, the simulations "feel" the chemical implications (e.g., enhanced air-sea gas exchange) due to rising atmospheric CO_2 but not the radiative/climate change impacts. In the first perturbation simulation (BGC, or biogeochemically coupled), C_{ant} invades the ocean, and its residence in the ocean impacts surface seawater chemistry and air-sea gas exchange. For conceptual purposes, C_{ant} at the ocean's surface is assumed to reflect both the direct C_{ant} invasion flux and reemerged C_{ant}. In the second simulation we implement a "hard suppression" of reemergence (RE_OFF) by maintaining preindustrial sea surface CO_2 partial pressure (pCO_2). This assumes that all obducting water masses are from interior reservoirs with no memory of the anthropogenic CO_2 transient. As such, the Revelle factor of surface waters is maintained at its preindustrial level. We consider this to be an idealized perturbation that provides a strong or upper-bound perturbation appropriate for testing the sensitivity of ocean CO_2 uptake in the absence of both reemergence and instantaneous subduction of C_{ant}.

2.2. The Ocean Carbon Cycle Model and Technical Implementation of Experimental Design

The ocean model configuration applied here is Version 5 of the Modular Ocean Model (MOM5; Griffies, 2009), in concert with the marine Biogeochemistry with Light Iron Nutrient and Gas model BLING (Galbraith et al., 2011). MOM5 has a nominal 1° horizontal resolution with 50 vertical levels. The model was spun up with the CORE Corrected Normal Year Forcing Version 2.0 (Large & Yeager, 2009) with a repeating seasonal cycle for 5,000 yr, with a fixed atmospheric CO_2 boundary condition (mixing ratio) of 286 μatm, until the globally integrated net air-sea CO_2 flux satisfied a drift threshold of <2 PgC per 240 yr.

Given our interest in prescribing CO_2 emissions, we have implemented a single well-mixed box reservoir (originally implemented in Sarmiento et al., 2010) to represent the atmospheric pCO_2 boundary condition for the ocean biogeochemistry model. Additionally, the net flux of CO_2 into the land (encompassing

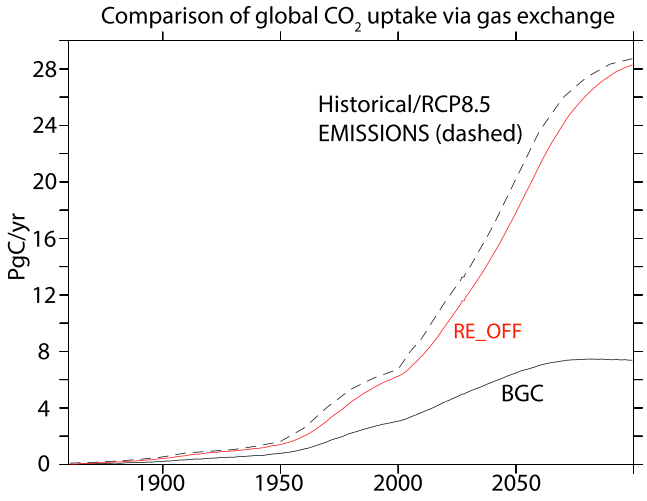

Figure 1. Globally integrated ocean CO_2 uptake from gas exchange using MOM5-BLING (Griffies, 2009; Galbraith et al., 2011) for BGC (solid black), RE_OFF (solid red), and historical/RCP8.5 emissions (dashed black).

uptake of anthropogenic emissions and land use change) is not accounted for in the historical/RCP8.5 emissions used here, so that the total inventory of the ocean and atmosphere inventories is conserved apart from emissions.

The simulations represent a single dynamical realization over the 1860–2099 period, but with three concurrent instances of the BLING biogeochemistry model (Galbraith et al., 2011) run online. The first instance represents the preindustrial control simulation (PI) over the interval 1860–2099, with an initial mixing ratio for CO_2 of 286 μatm in the well-mixed atmospheric reservoir box. The second instance (BGC) is fully prognostic and transient, following the historical/RCP8.5 emissions scenario (for gas exchange but not atmospheric radiative responses), with reemergence of properties to the surface allowed. The third instance (RE_OFF) is using the same historical/RCP8.5 emissions scenario as the BGC simulation but for which a suppression of reemergence and instantaneous subduction below the mixed layer of properties important for carbon exchange with the atmosphere was applied. This is accomplished by using a data override feature, allowing simulated sea surface DIC, TA, phosphate (PO_4), and silicate (SiO_4) concentrations from the PI run to be used in the calculation of pCO_2 within the gas exchange routines for RE_OFF on the time step level.

The contrast in global ocean CO_2 uptake between the RE_OFF and BGC simulations allows us to quantify the degree to which transients in the CO_2 buffering capacity of surface waters are important. To evaluate how the chemical component of marine carbon cycle feedbacks influences the overall physical climate system, we explore how the airborne fraction (AF) of anthropogenic CO_2 (Keeling et al., 1995) evolves in simulations where only marine chemistry is perturbed. The PI simulation makes it possible to define C_{ant} components for both the RE_OFF and BGC simulations through a simple differencing.

2.3. The AF and Climate Implications

Another question to consider is how the buffering capacity of the surface ocean impacts atmospheric CO_2 and thereby the radiative balance of the atmosphere and the climate system. For this we consider the cumulative airborne fraction (ΔCAF), defined here as the fraction of emissions over a specified time interval that remains in the atmosphere:

$$\Delta\mathrm{CAF} = \frac{\Delta \mathrm{CO_2}}{\Delta Q_E} \tag{1}$$

where ΔCO_2 represents the perturbation atmospheric inventory of CO_2 (in GtC; relative to preindustrial levels), and ΔQ_E (in GtC) represents cumulative anthropogenic emissions (Raupach, 2013). This definition differs from that typically used for AF (e.g., Canadell et al., 2007), where annual budgets are considered (annual accumulated fraction of CO_2 in the atmosphere versus annual carbon emissions).

Using ΔCAF enables an expansion of the TCRE:

$$\mathrm{TCRE} = \frac{\Delta \mathrm{SAT}}{\Delta Q_E} = \frac{\Delta \mathrm{SAT}}{\Delta \mathrm{CAF}} \cdot \frac{\Delta \mathrm{CAF}}{\Delta Q_E} \tag{2}$$

where ΔSAT represents globally averaged surface air temperature change. The first product term on the right-hand side of Equation 2, namely ΔSAT/ΔCAF, would encompass processes and feedbacks (e.g., cloud feedbacks) within the physical climate system, and it is this first product term that is typically the focus of TCRE research (Gillet et al., 2013). However, it is the second product on the right-hand side of Equation 2, namely $\Delta CAF/\Delta Q_E$, that we wish to investigate in this study. This term makes explicit the quantity of C_{ant} emitted that resides in the atmosphere, accounting for changes in the atmospheric inventory due to carbon fluxes from both land and ocean processes. Here by design, our focus is on the

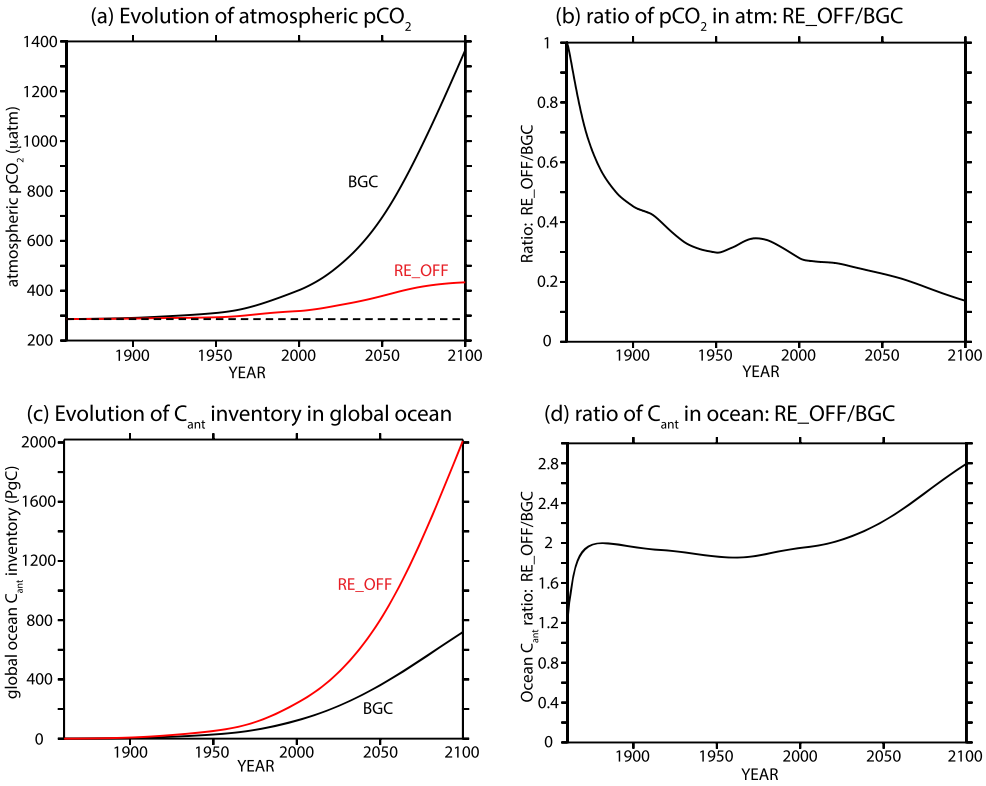

Figure 2. (a) Evaluation of atmospheric pCO_2 for BGC (solid black), RE_OFF (solid red), and PI (dashed black); (b) ratio of RE_OFF/BGC in atmospheric pCO_2 as a function of time; (c) evolution of globally integrated C_{ant} inventory in the ocean for BGC (black) and RE_OFF (red) (PgC); (d) ratio of RE_OFF/BGC in globally integrated C_{ant} inventory in the ocean.

signature of changes in the CO_2 buffering capacity of seawater as a response to our idealized perturbation, and so ΔCAF changes only through interaction with the ocean.

3. Results

3.1. Perturbations to Atmospheric and Oceanic Carbon Content

We first consider the globally integrated, annual mean air-sea CO_2 fluxes (Figure 1) for the BGC (solid black line) and RE_OFF (solid red line) simulations, along with the emissions flux (dashed black line). The CO_2 ocean uptake rate for RE_OFF is much larger than that of BGC over much of the 1860–2099 period, nearly keeping pace with emissions. From this analysis alone, it can be seen that the ocean uptake rate for BGC nears a leveling-off or saturation during the second half of the 21st century, whereas this does not occur for RE_OFF. As a consequence, we infer qualitatively that the ratio of RE_OFF to BGC ocean uptake increases over the 21st century. The evolution of the pCO_2 mixing ratio in the atmospheric reservoir is shown in Figure 2a. In the BGC simulation (solid black line) pCO_2 increases to 1,358 µatm by the end of the 21st century. The RE_OFF simulation (red line), in comparison, exhibits a significantly smaller increase than BGC in atmospheric pCO_2, reaching only 433 µatm by the Year 2099. The ratio of the atmospheric pCO_2 perturbations (RE_OFF/BGC) for the simulations (Figure 2b) illustrates that the perturbation for RE_OFF is 14% of the BGC perturbation by the Year 2099. The evolution of the full ocean inventory of C_{ant} is shown in Figure 2c, with the ratio of RE_OFF/BGC (Figure 2d) being approximately a factor of 2 over recent decades (1990–2010) and increasing to 2.8 by the Year 2099, consistent with the fluxes shown in Figure 1.

We now consider the evolution of BGC atmospheric pCO_2 (Figure 2a) and globally integrated C_{ant} inventories (Figure 2c) in light of observational constraints. The simulated global ocean inventory of C_{ant} in 1995 of 110 PgC falls within the uncertainty range of 118 ± 19 PgC from Sabine et al. (2004), based on

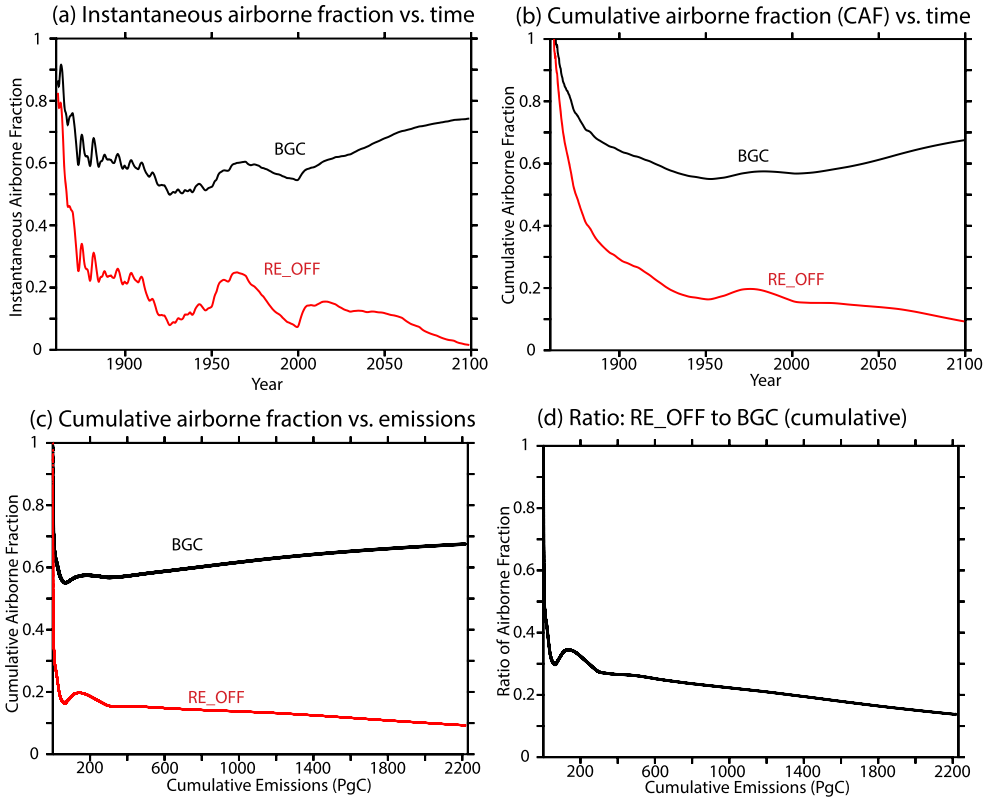

Figure 3. (a) Instantaneous airborne fraction of anthropogenic CO_2 emissions as a function of time for BGC (solid black) and RE_OFF (solid red); (b) cumulative airborne fraction of anthropogenic CO_2 emissions as a function of time for BGC (solid black) and RE_OFF (solid red); (c) cumulative airborne fraction of anthropogenic CO_2 emissions as a function of time for BGC (solid black) and RE_OFF (solid red); (d) ratio of RE_OFF/BGC for cumulative airborne fraction of anthropogenic CO_2 emissions as a function of emissions.

bottle data from the GLobal Ocean Data Analysis Project for Carbon (GLODAP) (Key et al., 2004) for the same time. However, the simulated atmospheric pCO_2 of 391 μatm is 40% higher (relative to preindustrial levels) than the observed level of 361 μatm in 1995 (http://www.esrl.noaa.gov/gmd/ccgg/trends/). Some of this discrepancy is resolved in light of an analogous run with the same ocean carbon cycle model forced with observed atmospheric pCO_2 (instead of CO_2 emissions) over the same period (Zhai et al., 2017), where the global ocean C_{ant} inventory is only 91 PgC in 1995, thereby reflecting a 20% low bias in model uptake with prescribed atmospheric pCO_2. We thereby interpret the simulated 40% high bias in atmospheric pCO_2 in 1995 for BGC as reflecting the combined effects of the low bias in ocean carbon uptake and the fact that our model configuration has no representation of terrestrial carbon uptake, with the observational constraints reported by Friedlingstein et al. (2019) indicating ~1 PgC/yr of terrestrial uptake over the time interval of interest.

3.2. The AF of CO_2 for the Atmosphere and Ocean

The evolution of the instantaneous AF simulated for the RE_OFF (red line) and BZGC (black line) experiments as a function of time is shown in Figure 3a. Over nearly the entire time interval RE_OFF is significantly smaller than BGC, with the ratio falling from 20% for the modern era to 2% by the end of the 21st century. This is reflected in the relationship in Figure 1 where ocean uptake for RE_OFF nearly keeps up with the instantaneous emissions rate over the full interval 1860–2099, with the ability of uptake to track emissions increasing in time. The decadal-time scale fluctuations in AF are also best understood with respect to modulations of the rate at which emissions increase with time over 1860–2099. For example, the increase in the rate of emissions during the 1950s is reflected in an increase in AF through time, while the decrease in the rate of emissions increases during the 1970s is reflected in a decrease in AF at that time. In order to

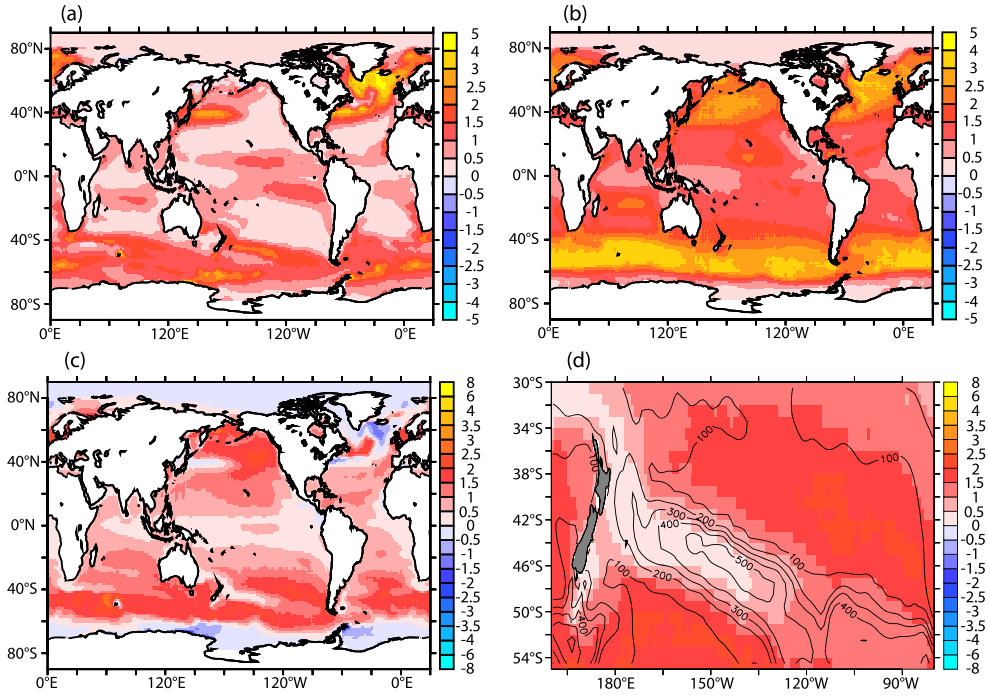

Figure 4. Air-sea fluxes of anthropogenic CO_2 averaged over 2000–2009 for (a) the difference between BGC and PI for air-sea CO_2 fluxes; (b) the difference between RE_OFF and PI; (c) the difference between RE_OFF and BGC; positive values indicate fluxes into the ocean, in units of moles m^{-2} yr^{-1}; and (d) superposition of the difference in air-sea CO_2 fluxes of anthropogenic CO_2 between RE_OFF and BGC (colors), with winter mixed layer depth (m) superposed (contours), revealing mixed layer depths in excess of 500 m in the region of minimum CO_2 flux differences.

evaluate our model against data-based estimates of AF, we consider the averaged AF over 1990–2006 of 46% identified by Canadell et al. (2007). For our model, we simulate an average AF over 1990–2006 of 56%, which is 20% higher than the data-based estimate in relative terms. However, if we impose in postprocessing a 1 PgC/yr net flux of CO_2 into the land, which is not explicitly simulated here, over 1990–2006 (consistent with the uncertainty estimates of Friedlingstein et al., 2019), our AF becomes 45%, in good agreement with the observationally based value.

The CAF considered over the full period (Figure 3b) for both BGC (black) and RE_OFF (red) has a significantly smoother distribution than AF over time, and the decline of RE_OFF is significantly less precipitous toward the end of the 21st century, dropping on 0.09 for the CAF as opposed to 0.02 for the AF. The CAF is shown as a function of cumulative emissions in Figure 3c, with this relationship corresponding to the second product term on the right-hand side of Equation 2. The ratio of RE_OFF to BGC is shown as a function of cumulative emissions in Figure 3d. Over the time interval 2000–2100, the ratio declines from approximately 0.25 to 0.14, reflecting the continually increasing rate of ocean uptake for RE_OFF and the leveling-off of ocean uptake for BGC (Figure 1).

Next, we consider the air-sea flux patterns of C_{ant} averaged over 2000–2009 at the air-sea interface for both the BGC simulation (BGC minus PI) (Figure 4a) and for the RE_OFF simulation (RE_OFF minus PI) (Figure 4b). The uptake of C_{ant} for BGC (Figure 4a) reveals features that are common to global carbon cycle simulations, with maximum uptake over both the Southern Ocean and the North Atlantic, including the western boundary currents and their extension regions (e.g., Frölicher et al., 2015). When integrated over large scales, the cumulative uptake between 45°S and 45°N over 1860–1995 accounts for approximately 60% of the global cumulative uptake, consistent with the modeling study of Iudicone et al. (2016). The uptake of C_{ant} for RE_OFF (Figure 4b) is significantly larger over global scales, and the spatial pattern differs. Over the Southern Hemisphere, there is maximum uptake of C_{ant} over the region ranging from the divergence (upwelling) at approximately 60°S to approximately 40°S. Over the Northern Hemisphere, uptake is maximum over the subpolar regions as well as over the northern subtropics. The difference in C_{ant} uptake

between the RE_OFF and BGC simulations (Figure 4c) reveals maxima over both 30–60°S and 30–60°N, except for the western boundary current regions. This is consistent with the latitude band over which Fassbender et al. (2017; their Figure 2b) argue that the Revelle factor values increase the most under the invasion flux of anthropogenic CO_2.

For the local minimum in CO_2 flux differences in the region directly to the east of New Zealand, we consider in Figure 4d the same field shown in Figure 4c but regionally, with wintertime mixed layer depths from the model superposed. This reveals that the minimum in CO_2 flux differences corresponds to the model's formation region for Subantarctic Mode Water (SAMW), namely, a water mass within a density class that is below that of the main thermocline. The SAMW formation process is interpreted to entrain deeper waters with little or no C_{ant}, and this accounts for sustaining the local minimum in the CO_2 flux difference. To the northeast of the region of maximum mixed layer depth near 120–110°W, 40–45°S the flux differences are maximum, consistent with the interpretation of Toyama et al. (2017) that reemergence of C_{ant} in thermocline density classes within the shallow overturning structures serves to inhibit C_{ant} uptake.

4. Discussion

When an extreme suppression of reemergence of C_{ant} from the ocean interior is imposed on a forward ocean circulation-carbon cycle model, the CAF as a function of cumulative carbon emissions is significantly reduced relative to the unperturbed case (Figure 3c), with the degree of reduction increasing in time (Figure 3d). By the end of the 21st century, the CAF with the RE_OFF perturbation is 17% of the CAF perturbation for the BGC case, representing a >900 μatm difference in atmospheric pCO_2. Viewed in terms of the TCRE, this reflects the amplitude of the second product term on the right-hand side of Equation 2 and is interpreted to represent the degree to which TCRE is amplified sevenfold by marine carbon cycle perturbations (relative to preindustrial). This sevenfold amplification occurs solely through anthropogenic modification of the buffering capacity of CO_2 in seawater.

Our experiments indicate that the changes in the buffering capacity regulate the carbon concentration feedback. This is consistent with previous studies (Arora et al., 2013; Williams et al., 2019) and provides an alternative framework for explicitly isolating and quantifying this chemical feedback. This positive chemical feedback dominates over the relatively modest 10% positive carbon-climate feedback (i.e., the influence of warming and physical state changes on the marine carbon cycle) derived from CMIP5 and CMIP6 models (Arora et al., 2020). Here we identify a 700% difference in the CAF for surface ocean chemical perturbations alone in the absence of changes to the physical state of the ocean. This has important implications for understanding mechanistically the transient climate sensitivity to cumulative CO_2 emissions. Given that GFDL's CMIP5-generation Earth system model ESM 2M (Dunne et al., 2012, 2013) exhibits a ~3.2°C globally averaged surface warming by 2100 under historical/RCP8.5 boundary conditions, and that the degree of warming is known to be close to proportionally related to the AF (Collins et al., 2013, IPCC), this implies that a significant fraction of the warming signal by the end of the 21st century is sustained through changes in the buffering capacity of CO_2 in the surface ocean. Perturbations to the physical state of the ocean under warming would be expected to modulate our results, as the Revelle factor declines with warming and salinification (as in Figure 1b of Fassbender et al., 2017). The question of the relationship between buffering capacity changes and surface ocean warming for the coupled system has been raised by Katavouta et al. (2018), Katavouta et al. (2019), and Williams et al. (2019), but further work will be required to identify the underlying mechanisms.

Perturbations to the buffering capacity of seawater and their connection to reemergence of C_{ant} are not explicitly quantified within the feedback diagnostics of Friedlingstein et al. (2003), as they are "hidden" within the beta term of that study. On the other hand, recent work (Katavouta et al., 2018) has argued within the TCRE framework that of order half of the transient climate sensitivity is in fact due to changes in the buffering capacity of the marine carbon cycle (i.e., the feedback is dominated by chemical rather than physical ocean perturbations) and advocated for a stronger role for the marine carbon cycle than what could be inferred from the work of Friedlingstein et al. (2003). It is our hope that the work presented here offers a mechanistic basis (via the role of C_{ant} reemergence) for reconciling the seeming discrepancies between these two tracks of research linking the marine carbon cycle and climate sensitivity. The negative (blue) difference regions reflect the fact that we have used an emissions rather than a concentration scenario, resulting in

higher atmospheric pCO_2 for RE_OFF than for BGC at any given time (Figure 2a). For the case of the Southern Ocean upwelling of very old waters in the divergence region near 60°S, with elevated preindustrial pCO_2 levels, there is thereby a net outgassing for RE_OFF that is larger than for BGC.

5. Conclusions

Our CMIP5-class ocean carbon cycle model has demonstrated that the net ocean uptake of C_{ant} is strongly sensitive to perturbations in the CO_2 buffering capacity of surface ocean waters. This is closely connected to the process of reemergence of C_{ant} from the ocean interior to the surface mixed layer (the mechanism highlighted by Toyama et al., 2017). For the idealized case we impose of instantaneous subduction of C_{ant} with zero reemergence over the duration of the experiment, the ocean is able to absorb substantially more carbon from the atmosphere than for the case with extensive reemergence, increasing the ocean carbon inventory by a factor of 2 over the 20th century and reaching a factor of 2.8 by the end of the 21st century.

For the atmospheric carbon reservoir, this corresponds to a significantly reduced CAF for the RE_OFF simulation. The CAF for the perturbed simulation is only 33% of the unperturbed simulation over recent decades, with this decreasing to 15% by the end of the 21st century. As was demonstrated in Equation 2, this has direct consequences for the TCRE within the Earth system. To put this into context, for the case where the Earth system is projected to warm by 3.5°C by the end of the 21st century under a business-as-usual emissions scenario, our results indicate as an upper bound that the 3.5°C warming reflects an amplification by a factor of 7 relative to a 0.5°C warming that would occur in the absence of changes to the buffering capacity of surface seawater. Differences in the simulated buffering capacity of CMIP5 and CMIP6 models may thereby contribute to differences in their intermodel spread in TCRE, due to differences in the renewal time scales of upper ocean waters.

Data Availability Statement

Model output is available through http://dogfish.princeton.edu/RODGERS_GRL_2020/.

Acknowledgments

The contribution of K. B. R. came through IBS-R028-D1. Support for M. I. and K. T. comes through MRI's research fund C4 for studies of ocean biogeochemistry and acidification and MEXT Kakenhi 19H05700. Support for S. S. and R. D. S. came through NASA Award NNX17A175G. T. L. F. acknowledges financial support from the Swiss National Science Foundation (PP00P2_170687) and the European Union's Horizon 2020 research and innovative program under Grant Agreement 820989 (project COMFORT. Our common future ocean in the Earth system—Quantifying coupled cycles of carbon, oxygen, and nutrients for determining and achieving safe operating spaces with respect to tipping points) for financial support. A. J. F. was supported by the David and Lucile Packard Foundation. O. Aumont would like to thank the PISCO project.

References

Arora, B. K., Boer, G. J., Friedlingstein, P., Eby, M., Jones, C. D., Christian, J. R., et al. (2013). Carbon-concentration and carbon-climate feedbacks in CMIP5 Earth system models. *Journal of Climate*, *26*, 5789–5314.

Arora, V. K., Katavouta, A., Williams, R. G., Jones, C. D., Brovkin, V., Friedlingstein, P., et al. (2020). Carbon–concentration and carbon–climate feedbacks in CMIP6 models and their comparison to CMIP5 models. *Biogeosciences*, *17*(16), 4173–4222. https://doi.org/10.5194/bg-17-4173-2020

Bolin, B., & Eriksson, E. (1959). Changes in the carbon dioxide content of the atmosphere and sea dude to fossil fuel combustion. In B. Bolin (Ed.), *The Atmosphere and the Sea in Motion* (130–142). New York: Rockefeller Inst. Press.

Canadell, J. G., le Quere, C., Raupach, M. R., Field, C. B., Buitenhuis, E. T., Ciais, P., et al. (2007). Contributions to accelerating atmospheric CO_2 growth from economic activity, carbon intensity, and efficiency of natural sinks. *Proceedings of the National Academy of Sciences of the United States of America*, *104*(47), 18,866–18,870. https://doi.org/10.1073/pnas.0702737104

Collins, M., Knutti, R., Arblaster, J., Dufresne, J.-L., Fichefet, T., Friedlingstein, P., et al. (2013). Climate change. In T. F. Stocker et al. (Eds.), *The Physical Science Basis* (pp. 1029–1136). Cambridge: IPCC, Cambridge Univ. Press.

Dunne, J. P., John, J. G., Adcroft, A. J., Griffies, S. M., Hallberg, R. W., Shevliakova, E., et al. (2012). GFDL's ESM 2 global coupled climate-carbon Earth system models. Part I: Physical formulation and baseline simulation characteristics. *Journal of Climate*, *25*(19), 6646–6665. https://doi.org/10.1175/JCLI-D-11-00560.1

Dunne, J. P., John, J. G., Shevliakova, E., Stouffer, R. J., Krasting, J. P., Malyshev, S. L., et al. (2013). GFDL's ESM 2 global coupled climate-carbon Earth system models. Part II: Carbon system formulation and baseline simulation characteristics. *Journal of Climate*, *26*, 2247–2267.

Fassbender, A. J., Sabine, C. L., & Palevsky, H. I. (2017). Nonuniform ocean acidification and attenuation of the ocean carbon sink. *Geophysical Research Letters*, *44*, 8404–8413. https://doi.org/10.1002/2017GL074389

Forster, P. M., Andrews, T., Good, P., Gregory, J. M., Jackson, L. S., & Zelinka, M. (2013). Evaluating adjusted forcing and model spread for historical and future scenarios in the CMIP5 generation of climate models. *Journal of Geophysical Research: Atmospheres*, *118*, 1139–1150. https://doi.org/10.1002/jgrd.50174

Friedlingstein, P., Cox, P., Betts, R., Bopp, L., von Bloh, W., Brovkin, V., et al. (2006). Climate-carbon cycle feedback analysis: Results from the C4MIP-model intercomparison. *Journal of Climate*, *19*(14), 3337–3353. https://doi.org/10.1175/JCLI3800.1

Friedlingstein, P., Dufresne, J. L., Cox, P. M., & Rayner, P. (2003). How positive is the feedback between climate change and the carbon cycle? *Tellus*, *55B*, 692–700.

Friedlingstein, P., Jones, M. W., O'Sullivan, M., Andrew, R. M., Hauck, J., Peters, G. P., et al. (2019). Global carbon budget 2019. *Earth System Science Data*, *11*(4), 1783–1838. https://doi.org/10.5194/essd-11-1783-2019

Frölicher, T. L., Sarmiento, J. L., Paynter, D. J., Dunne, J. P., Krasting, J. P., & Winton, M. (2015). Dominance of the Southern Ocean in anthropogenic carbon and heat uptake in CMIP5 models. *Journal of Climate*, *28*(2), 862–886. https://doi.org/10.1175/JCLI-D-14-00117.1

Galbraith, E. D., Kwon, E. Y., Gnanadesikan, A., Rodgers, K. B., Griffies, S. M., Dunne, J. P., et al. (2011). The impact of climate variability on the distribution of radiocarbon in CM2Mc, a new Earth system model. *Journal of Climate*, *24*(16), 4230–4254. https://doi.org/10.1175/2011JCLI3919.1

Gillet, N. P., Arora, V. K., Matthews, H. D., & Allen, M. R. (2013). Constraining the ratio of global warming to cumulative CO_2 emissions using CMIP5 simulations. *Journal of Climate*, *26*, 2844–2858.

Goodwin, P., Williams, R. G., & Ridgwell, A. (2015). Sensitivity to cumulative carbon emissions due to compensation of ocean heat and carbon uptake. *Nature Geoscience*, *8*(1), 29–34. https://doi.org/10.1038/ngeo2304

Griffies, S. M. (2009). Elements of MOM4p1. GFDL Ocean Group Tech. Rep. 6, p 37 [Available online at http://data1.gfdl.noaa.gov/~arl/pubrel/o/old/doc/mom4p1_guide.pdf].

Iudicone, D., Rodgers, K. B., Plancherel, Y., Aumont, O., Ito, T., Key, R., et al. (2016). The formation of the ocean's anthropogenic carbon reservoir. *Scientific Reports*, *6*(1), 35473. https://doi.org/10.1038/srep35473

Katavouta, A., Williams, R. G., & Goodwin, P. (2019). The effect of ocean ventilation on the transient climate response of emissions. *Journal of Climate*, *32*(16), 5085–5105. https://doi.org/10.1175/JCLI-D-18-0829.1

Katavouta, A., Williams, R. G., Goodwin, P., & Roussenov, V. M. (2018). Reconciling atmospheric and oceanic views of the transient climate response to emissions. *Geophysical Research Letters*, *45*, 6205–6214. https://doi.org/10.1029/2018GL077849

Keeling, C. D., Whorf, T. P., Wahlen, M., & Plichtt, J. V. D. (1995). Interannual extremes in the rate of rise of atmospheric carbon dioxide since 1980. *Nature*, *375*, 666–670. https://doi.org/10.1038/375666a0

Key, R. M., Kozyr, A., Sabine, C. L., Lee, K., Wanninkhof, R., Bullister, J., et al. (2004). A global ocean carbon climatology: Results from Global Data Analysis Project (GLODAP). *Global Biogeochemical Cycles*, *18*, GB4031. https://doi.org/10.1029/2004GB002247

Large, W. G., & Yeager, S. (2009). The global climatology of an interannually varying air-sea flux data set. *Climate Dynamics*, *33*(2–;3), 341–364. https://doi.org/10.1007/s00382-008-0441-3

Matthews, H. D., Gillet, N. P., Stott, P. A., & Zickfeld, K. (2009). The proportionality of global warming to cumulative carbon emissions. *Nature*, *459*, 820–832.

Raupach, M. R. (2013). The exponential eigenmodes of the carbon-climate system, and their implications for ratios of responses to forcings. *Earth System Dynamics*, *4*(1), 31–49. https://doi.org/10.5194/esd-4-31-2013

Revelle, R., & Suess, H. E. (1957). Carbon dioxide exchange between atmosphere and ocean and the question of an increase of atmospheric CO_2 during the past decades. *Tellus*, *9*, 1–10. https://doi.org/10.3402/tellusa.v9i1.9075

Rogelj, J., Forster, P. M., Kriegler, E., Smith, C. J., & Séférian, R. (2019). Estimating and tracking the remaining carbon budget for stringent climate targets. *Nature*, *571*(7765), 335–342. https://doi.org/10.1038/s41586-019-1368-z

Sabine, C. L., Feely, R. A., Gruber, N., Key, R. M., Lee, K., Bullister, J. L., et al. (2004). The oceanic sink for anthropogenic CO_2. *Science*, *305*(5682), 367–371. https://doi.org/10.1126/science.1097403

Sarmiento, J. L., Slater, R. D., Dunne, J., Gnanadesikan, A., & Hiscock, M. R. (2010). Efficiency of small-scale carbon mitigation by patch iron fertilization. *Biogeosciences*, *7*(11), 3593–3624. https://doi.org/10.5194/bg-7-3593-2010

Toyama, K., Rodgers, K. B., Blanke, B., Iudicone, D., Ishii, M., Aumont, O., & Sarmiento, J. L. (2017). Large reemergence of anthropogenic carbon into the ocean's surface mixed layer sustained by the ocean's overturning circulation. *Journal of Climate*, *30*, 8515–8631.

van Vuuren, D. P., Edmonds, J., Kainuma, M., Riahi, K., Thomson, A., Hibbard, K., et al. (2011). The representative concentration pathways: An overview. *Climatic Change*, *109*(1–2), 5–31. https://doi.org/10.1007/s10584-011-0148-z

Williams, R. G., Katavouta, A., & Goodwin, P. (2019). Carbon-cycle feedbacks operating in the climate system. *Current Climate Change Reports*, *5*(4), 282–295. https://doi.org/10.1007/s40641-019-00144-9

Zhai, P., Rodgers, K. B., Griffies, S. M., Slater, R. D., Iudicone, D., Sarmiento, J. L., & Resplandy, L. (2017). Mechanistic drivers of reemergence of anthropogenic carbon in the equatorial Pacific. *Geophysical Research Letters*, *44*, 9433–9439. https://doi.org/10.1002/2017GL073758